Eur. Phys. J. C 18, 547–553 (2001)
Digital Object Identifier (DOI) 10.1007/s100520000546

THE EUROPEAN PHYSICAL JOURNAL C

Variable flavor number schemes versus fixed order perturbation theory for charm quark electroproduction

A. Chuvakin[1], J. Smith[1], B.W. Harris[2]

[1] C.N. Yang Institute for Theoretical Physics, State University of New York at Stony Brook, Stony Brook, NY 11794-3840, USA
[2] High Energy Physics Division, Argonne National Laboratory, Argonne, IL 60439, USA

Received: 31 October 2000 / Revised version: 8 November 2000 /
Published online: 21 December 2000 – © Springer-Verlag 2000

Abstract. Data for $D^{*\pm}(2010)$ meson electroproduction in the range $10 < Q^2 < 1350$ GeV^2 has recently been presented by the ZEUS collaboration at HERA. We use these results together with previously published data for $Q^2 > 1$ GeV^2 to test whether one can distinguish between different theoretical schemes for charm quark electroproduction. We find that up to the largest Q^2 measured, it is not possible to make such a differentiation. Then we point out the regions where differences between the various schemes arise.

1 Introduction

Electromagnetic interactions have long been used to study both hadronic structure and strong interaction dynamics. Examples include deep inelastic lepton-nucleon scattering, hadroproduction of lepton pairs, the production of photons with large transverse momenta, and various photoproduction processes involving scattering of real or very low mass virtual photons from hadrons. In particular, heavy quark production in deep inelastic electron-proton scattering is calculable in QCD and provides information on the gluonic content of the proton which is complementary to that obtained in direct photon production or structure function scaling violation measurements. In addition, the scale of the hard scattering may be large relative to the mass of the charm quark, thus allowing one to study whether and when to treat the charm quark as a massless parton. It is this second aspect we wish to examine further in this paper.

The photon-gluon fusion mechanism is the simplest description of charmed quark electroproduction so that their production is assumed extrinsic, and their mass m_c is retained throughout. We call this description fixed order perturbation theory (FOPT). It depends on a three-flavor set of parton densities for the u, d, and s quarks together with a corresponding gluon density. Calculations for rates and single particle inclusive distributions are available to next-to-leading order (NLO) in [1]. These calculations were later redone to cover fully differential production [2], and decays into hadronic or semileptonic final states [3]. This framework generally provides a very good description of the ZEUS [4] and H1 data [5] on the differential distributions for $D^{*\pm}(2010)$ electroproduction. Updated analyses now exist from H1 [6] and ZEUS [7]. The ZEUS data [7] now extend up to $Q^2 \approx 1000$ GeV^2. Since the FOPT results in NLO are very stable under scale changes it has been advocated that a three-flavor description should be the best one to fit the data [8,9]. This is the reason that the GRV98 leading order (LO) and NLO density sets [10] only contain three flavors.

Other descriptions of charm quark electroproduction have been used. One, which describes the charm quark as a massless parton density $c(x,\mu^2)$, with the boundary condition $c(x,\mu^2) = 0$ for $\mu \leq m_c$, is expected to be more appropriate at large Q^2. This scheme has generally been used by groups which fitted parton densities to data and is called the zero-mass variable flavor number scheme (ZM-VFNS). The transition from a three-flavor parton density set to a four-flavor set can be made on purely theoretical grounds by evaluating appropriate massive and massless operator matrix elements containing heavy quark loops in the operator product expansion and then absorbing the terms containing $\ln^i(Q^2/m_c^2)$ into the definition of four-flavor parton densities [11], [12]. The resummation of the above logarithms is incorporated into the boundary conditions on the $c-$quark density as well as the other four-flavor quark and gluon densities. In particular if one does this at the scale where $\mu^2 = Q^2 = m_c^2$ then all the logarithmic terms in the operator matrix elements vanish and only the non-logarithmic terms are included in the boundary conditions. Since a charm quark density is a parton model concept the QCD perturbation series then starts with α_s^0 coefficient functions. The lowest order photon-gluon fusion reaction then has $O(\alpha_s)$ coefficient functions. The NLO corrections contain $O(\alpha_s^2)$ coefficient functions. When the resulting four-flavor parton densities are convolved with the massless coefficient functions in [13] one obtains predictions for the charm content in the deep in-

elastic structure functions. One expects this four-flavor ZM-VFNS description to be better than the FOPT one at large scales since it resums the terms in $\ln^i(Q^2/m_c^2)$.

Another approach, which is even more ambitious, is a scheme designed to interpolate between the FOPT result at low scales and the ZM-VFNS result at large scales. In these variable flavor number schemes (VFNS) one hopes to provide a unified framework for all scales. Unfortunately there is no unique prescription for a VFNS and several have been constructed. The differences between them are due to two inputs. The first is the mass factorization procedure carried out before the large logarithms can be resummed, namely should one retain massive or massless charmed quarks in the coefficient functions, which are convolved with either the three-flavor or four-flavor parton densities. The second is the matching condition imposed on the charmed quark density, namely how does it vanish in the threshold region of the electroproduction process, where the partonic subenergy is approximately $4m_c^2$. Variable flavor number schemes are presently available to $O(\alpha_s)$ in [14–17] and to $O(\alpha_s^2)$ in [18,19], called BMSN and CSN, respectively, in this paper. The latter schemes require the parton densities provided in [12]. Review articles and discussions about VFNS schemes are available in [20–23].

In Sect. 2 we give a short discussion of the BMSN and CSN descriptions for charmed quark electroproduction and then compare theoretical predictions with differential distribution data from H1 [6] and ZEUS [4,7].

2 Comparison

The reaction under consideration is heavy quark Q production via neutral-current electron-proton scattering

$$e^-(l) + P(p) \to e^-(l') + Q(p_1) + X. \tag{2.1}$$

We concentrate on the case where Q is a charm quark with mass $m_c = 1.4$ GeV. When the momentum transfer squared $Q^2 = -q^2 > 0$ ($q = l - l'$) is not too large, $Q^2 \ll M_Z^2$, the contribution from virtual Z-boson exchange is small compared to that of virtual-photon exchange. For example, using the leading order Monte Carlo program AROMA [24], at $Q^2 = 1000$ GeV^2 we find the Z-boson exchange contribution is a factor of 100 smaller than the photon exchange contribution.

The charm quark cross section can be written in terms of the structure functions $F_2^c(x, Q^2, m_c^2)$ and $F_L^c(x, Q^2, m_c^2)$ as follows:

$$\frac{d^2\sigma}{dydQ^2} = \frac{2\pi\alpha^2}{yQ^4}\{[1 + (1-y)^2]F_2^c(x, Q^2, m_c^2) - y^2 F_L^c(x, Q^2, m_c^2)\}, \tag{2.2}$$

where $x = Q^2/2p \cdot q$ and $y = p \cdot q/p \cdot l$ are the usual Bjorken scaling variables and α is the electromagnetic coupling. The scaling variables are related to the square of the center-of-momentum energy of the electron-proton system $S = (l+p)^2$ *via* $xyS = Q^2$. The total cross section is given by [25]

$$\sigma = \int_{4m_c^2/S}^1 dy \int_{m_e^2 y^2/(1-y)}^{yS-4m_c^2} dQ^2 \left(\frac{d^2\sigma}{dydQ^2}\right), \tag{2.3}$$

where m_e is the electron mass. In deriving (2.2) one integrates over the azimuthal angle between the plane containing the incoming and outgoing electrons and the plane containing the incoming proton and the outgoing charm quark.

Experimentally it is the decay products of charmed hadrons that are observed. The H1 and ZEUS groups measure $D^{*\pm}(2010)$ production. We assume a Peterson *et al.* [26] fragmentation function to model the nonperturbative transition from charmed quark to hadron. The cross section for D^* production is then obtained by convolving the charm quark cross section (2.3) with the fragmentation function

$$D(z) = \frac{N}{z[1 - 1/z - \epsilon/(1-z)]^2} \tag{2.4}$$

where N is fixed such that $D(z)$ is normalized to unity once the parameter $\epsilon = 0.035$ [27] is fixed. The normalization of the cross section is then given by the charm fragmentation probability which we take as $P(c \to D^*) = 0.235$ [28].

The H1 Collaboration has recently [6] measured $D^{*\pm}$ production for $1 < Q^2 < 100$ GeV^2 and $0.05 < y < 0.7$ and quote a cross section in the region $1.5 < p_T(D^*) < 15$ GeV and $|\eta(D^*)| < 1.5$ of

$$\sigma(e^+p \to e^+D^{*\pm}X) = 8.37 \pm 0.41(\text{stat.})^{+1.11}_{-0.82}(\text{syst.})\ \text{nb}. \tag{2.5}$$

The data came from the 1996-97 run with proton energy 820 GeV and positron energy 27.5 GeV (18.6 pb^{-1}).

The ZEUS Collaboration has recently [7] measured $D^{*\pm}$ production for $Q^2 > 10$ GeV^2 and $0.04 < y < 0.95$ and quote a cross section in the region $1.5 < p_T(D^*) < 15$ GeV and $|\eta(D^*)| < 1.5$ of

$$\sigma(e^+p \to e^+D^{*\pm}X) = 2.33 \pm 0.12(\text{stat.})^{+0.14}_{-0.07}(\text{syst.})\ \text{nb}. \tag{2.6}$$

The data came partly from the 1999-2000 run with proton energy 920 GeV (45.0 pb^{-1}) and partly from the 1995-1997 run with proton energy 820 GeV (37.6 pb^{-1}). In both cases the positron beam energy was 27.6 GeV. They demonstrated [7] that the predictions from HVQDIS [3], which is based on FOPT, agree with their $D^{*\pm}$ electroproduction data up to the highest measured value of $Q^2 \approx 1350$ GeV^2.

Previously in [4] they presented the 1996-1997 positron production data (37 pb^{-1}) for $D^{*\pm}$ in the range $1 < Q^2 < 600$ GeV^2 and $0.02 < y < 0.7$ in the same kinematic range $1.5 < p_T(D^*) < 15$ GeV and $|\eta(D^*)| < 1.5$ with the cross section

$$\sigma(e^+p \to e^+D^{*\pm}X) = 8.31 \pm 0.31(\text{stat.})^{+0.30}_{-0.50}(\text{syst.})\ \text{nb}. \tag{2.7}$$

Therein [4] they also concluded that the HVQDIS [3] results agree with their data, apart from a distortion of the pseudo-rapidity distribution. This was attributed to a beam drag effect [29], which was estimated by Monte Carlo [30]. Still FOPT seemed to be the best model to fit their data.

The BMSN [18] and CSN [19] variable flavor number schemes were constructed so that the charm quark structure functions $F_2^c(x,Q^2,m_c^2,\mu^2)$ and $F_L^c(x,Q^2,m_c^2,\mu^2)$ are numerically equal to the corresponding FOPT results at the scale $\mu^2 = m_c^2 = Q^2 = 1.96$ GeV^2, so the differences between the them could be monitored at higher scales. For this reason we chose the scale $\mu^2 = m_c^2 + \frac{1}{2}Q^2(1-m_c^2/Q^2)^2$ and set the charm density to zero when $\mu^2 < m_c^2$. Also we used the exact solution of the differential equation for the QCD running coupling (α_s) as well as an electromagnetic running coupling (α). The QCD expansion was truncated at α_s^2. Therefore we were careful to construct the structure functions in the FOPT, BMSN and CSN schemes according to the symbolic formula

$$\begin{aligned} &F(x,Q^2,m_c^2) \\ &= f(LO)\otimes C(LO) \\ &\quad +\alpha_s[f(NLO)\otimes C(LO) + f(LO)\otimes C(NLO)] \\ &\quad +\alpha_s^2[f(LO)\otimes C(NNLO) + f(NLO)\otimes C(NLO) \\ &\quad +f(NNLO)\otimes C(LO)]\,, \end{aligned} \tag{2.8}$$

where the $\otimes$ symbol refers to the convolution integral and the parton densities f and coefficient functions C are taken in either LO, NLO or next-to-next-to-leading order (NNLO) perturbation theory. Note that this result is different from the usual FOPT prescription which is based on expressions like

$$\begin{aligned} &F(x,Q^2,m_c^2) \\ &= [f(LO)+\alpha_s f(NLO)+\alpha_s^2 f(NNLO)] \\ &\quad \otimes[C(LO)+\alpha_s C(NLO)+\alpha_s^2 C(NNLO)]\,. \end{aligned} \tag{2.9}$$

These prescriptions retain terms which are even higher order in α_s. Normally it does not matter if such terms are retained because they are numerically unimportant at large Q^2. However such terms are numerically significant at small Q^2 and ruin the cancellations among the various terms in our formulae for the structure functions in the three schemes with the result that they do not agree numerically at $Q^2 = \mu^2 = m_c^2$. Therefore we have to use (2.8) and not (2.9). Even our FOPT (extrinsic) expression, called EXACT in this paper, only retains the second and third sets of terms in (2.8) and agrees with the corresponding results from the (appropriately modified) HVQDIS code.

The difference between the BMSN and CSN schemes is that the former has $m_c = 0$ in the heavy quark coefficient functions while the latter retains terms containing m_c. We refer the reader to [19] for more details, in particular the definition of the collinear safe inclusive structure functions and the contributions which are incorporated into the light mass (u,d,s) contributions to the coefficient functions. Our previous theoretical results showed that differences between the EXACT, BMSN and CSN schemes in LO perturbation theory diminish substantially in NLO perturbation theory. Such differences are more apparent for b-quark electroproduction in [31] but there are no events yet.

The aim of this paper is to compare our results with the data. Since there are no VFNS schemes available for differential distributions in the transverse momentum and rapidity of the D^* meson in $O(\alpha_s^2)$ we make the assumption that the experimental acceptances do not differ much between these schemes and FOPT. We have therefore recalculated the experimental acceptances from the HVQDIS program with the above scale choice, running coupling constant and GRV98 [10] three-flavor parton density set. This is appropriate for the FOPT result, which we called EXACT in our papers on the BMSN and CSN schemes. Our acceptances in Q^2 are slightly modified from those used by the Collaborations. The acceptances in Q^2, from integrating (2.2) over $0.04 < y < 0.95$, $0.05 < y < 0.7$, or $0.02 < y < 0.7$ are nearly identical, so we do not distinguish between them. The corresponding acceptances in x, however, from integrating (2.2) over $10 < Q^2 < 1350$ or $1 < Q^2 < 600$ and the corresponding y ranges are different and we distinguish between them. We start with the recent data from the Osaka meeting [6,7]. The results for the ratio $\sigma(\text{cuts})/\sigma(\text{no cuts})$ are presented in Figs. 1 and 2 plotted versus $\log_{10}Q^2$ and $\log_{10}x$ respectively. These plots demonstrate the large corrections necessary to include the experimental acceptances. The corrections were applied to the corresponding differential cross sections calculated from the structure functions given in the CSN [19] and BMSN [18] papers. Here we used our own set of densities [12] which are based on the three-flavor GRV98 densities at scales below $\mu = m_c$, but which incorporate the discontinuity across the $c-$flavor threshold at $\mu = m_c$ to define a four-flavor set both in $O(\alpha_s)$ and in $O(\alpha_s^2)$ together with their subsequent evolution to higher scales with NLO splitting functions.

The resulting differential cross sections in $\log_{10}Q^2$ are compared with the H1 and ZEUS data in Figs. 3 and 4. We see from Fig. 3 that the FOPT is a good fit to the data at large Q^2. This is in agreement with the conclusions of the ZEUS Collaboration in [7]. It is difficult to distinguish the BMSN and CSN results from the FOPT ones because there is only a 4% difference even at this large Q^2. Clearly it will take a substantial increase in the number of events to distinguish between the schemes at large Q^2. All we can say at present is that the terms containing powers of $\ln(Q^2/m_c^2)$ do not seem to lead to different predictions.

One can see from the semi-logarithmic plot in Fig. 4 that all curves meet at $Q^2 = m_c^2 = 1.96$ GeV^2, which is expected from the construction of the BMSN and CSN schemes. There are differences between the three schemes in the region of small Q^2, however the currently available data is unable to resolve them. We understand that the events with $Q^2 < 10$ GeV^2 and with $Q^2 > 10$ GeV^2 are measured in different regions of the ZEUS detector and the events accumulated in 1999-2000 in the former region have not been analyzed. Note also that the bin widths

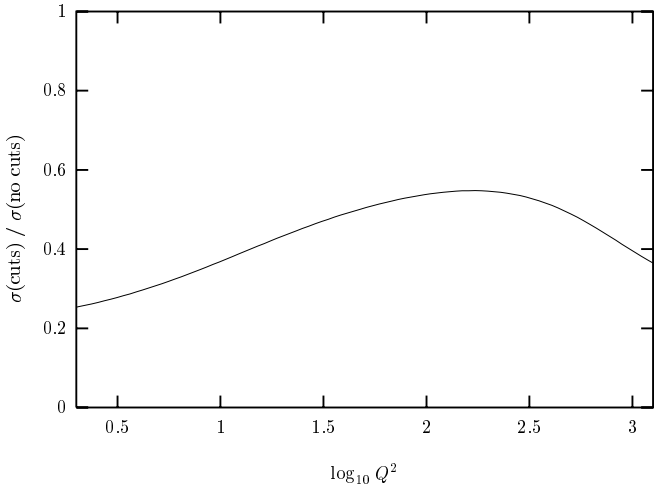

Fig. 1. The ratio $\sigma(\text{cuts})/\sigma(\text{no cuts})$ for the acceptance in Q^2 plotted versus $\log_{10}Q^2$

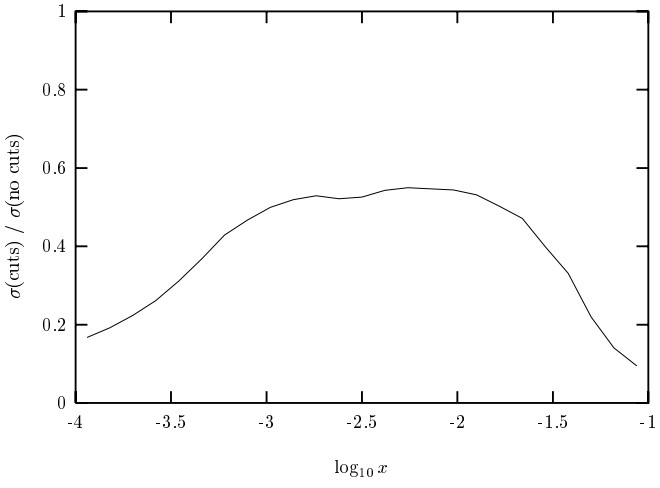

Fig. 2. The ratio $\sigma(\text{cuts})/\sigma(\text{no cuts})$ for the acceptance in x plotted versus $\log_{10}x$

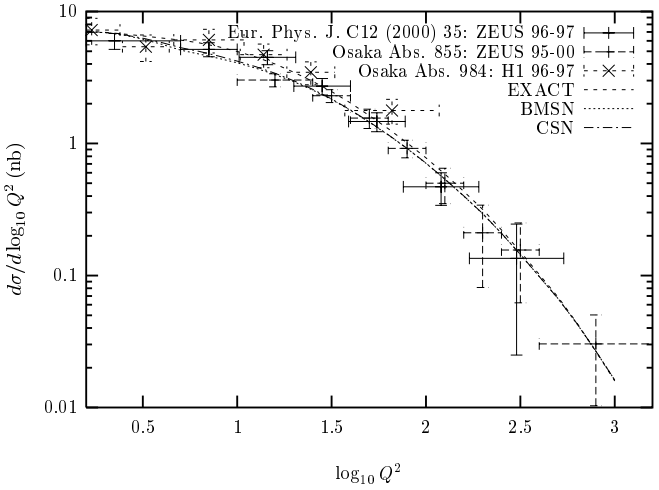

Fig. 3. The combined Osaka H1 and ZEUS and published ZEUS data for $d\sigma/d\log_{10}Q^2$ in nb for deep inelastic production of $D^{*\pm}$ mesons. The dashed line is the NLO EXACT result from HVQDIS, (which coincides with the FOPT result), the dotted line is the result from the BMSN scheme and the dot-dashed line is the result from the CSN scheme

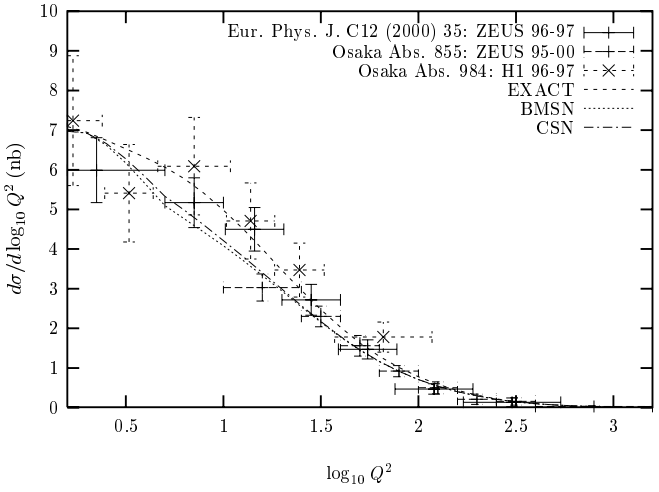

Fig. 4. Same as Fig. 3 displayed on a semi-logarithmic plot

in this region are not the same. More data for small Q^2 would clearly be very useful.

The resulting differential cross sections in $\log_{10}x$ are compared with the new ZEUS data [7] in Figs. 5 and 6. We see from Fig. 5 that there is good agreement over a wide range in x. The semi-logarithmic plot in Fig. 6 shows a small disagreement between the FOPT theory result and the data in the region $x \approx 10^{-3}$. However the normalization is determined mainly by the magnitude of differential cross section at the lowest measured point in Q^2, which is precisely where additional data is required.

Integrations over the theoretical results displayed in Figs. 3–6 for $10 < Q^2 < 1350$ GeV^2 and $0.04 < y < 0.95$ yield 2.86 nb, 2.51 nb and 2.48 nb for the FOPT, BMSN and CSN schemes respectively. The latter two results are within the error bars of the experimental result in (2.6) while the FOPT result is slightly higher.

The previous published ZEUS data in [4] had different cuts in Q^2 and y, namely $1 < Q^2 < 600$ GeV^2 and $0.02 < y < 0.7$ which affect the normalization of the corresponding x distribution. Therefore we reran the acceptance in $\log_{10}x$ from the HVQDIS program and it is shown in Fig. 7. We then applied the same acceptance to the other programs. The BMSN and CSN results between $1 < Q^2 < 1.96$ GeV^2 are set equal to the EXACT result. Our results are compared to the data in Figs. 8 and 9. The overall shape and normalization are well described. Integration over the results in Fig. 8 yield 9.29 nb, 8.43 nb and 8.55 nb for the FOPT, BMSN and CSN schemes respectively compared to the experimental results in (2.5) and (2.7).

We have run our computer codes in other ranges of the variables $\log_{10}Q^2$ and $\log_{10}x$ to find where differences between the three schemes might be measurable. As an illustration we show in Fig. 10 a contour plot of the ratio of the BMSN double differential cross section divided by the FOPT double differential cross section plotted versus

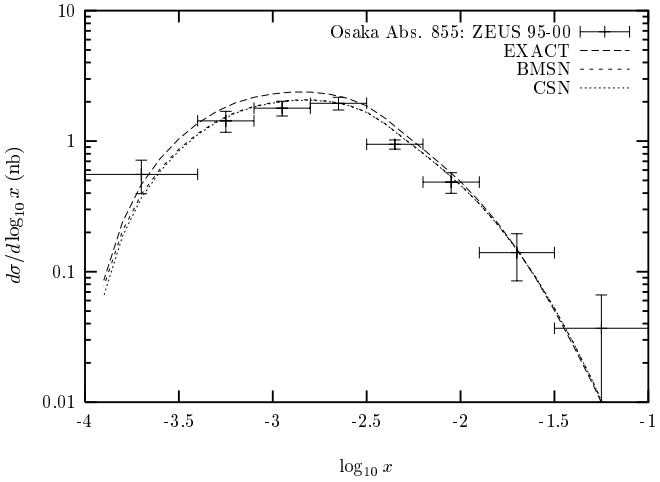

Fig. 5. The Osaka ZEUS data for $d\sigma/d\log_{10}x$ in nb for deep inelastic production of $D^{*\pm}$ mesons. The dashed line is the NLO EXACT result from HVQDIS, (which coincides with our FOPT result), the dotted line is the result from the BMSN scheme and the dot-dashed line is the result from the CSN scheme

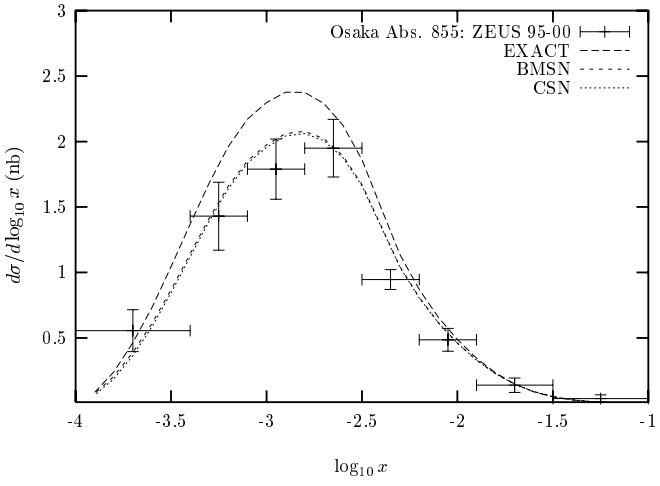

Fig. 6. Same as Fig. 5 displayed on a semi-logarithmic plot

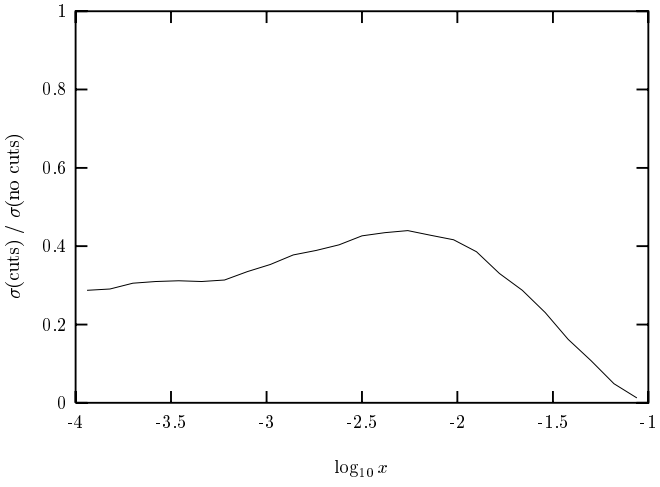

Fig. 7. The ratio $\sigma(\text{cuts})/\sigma(\text{no cuts})$ for the acceptance in x plotted versus $\log_{10}x$

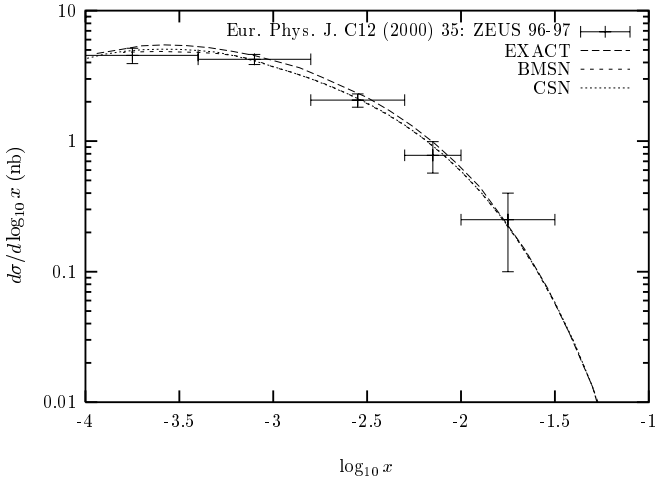

Fig. 8. The published ZEUS data for $d\sigma/d\log_{10}x$ in nb for deep inelastic production of $D^{*\pm}$ mesons. The notation follows Fig. 5

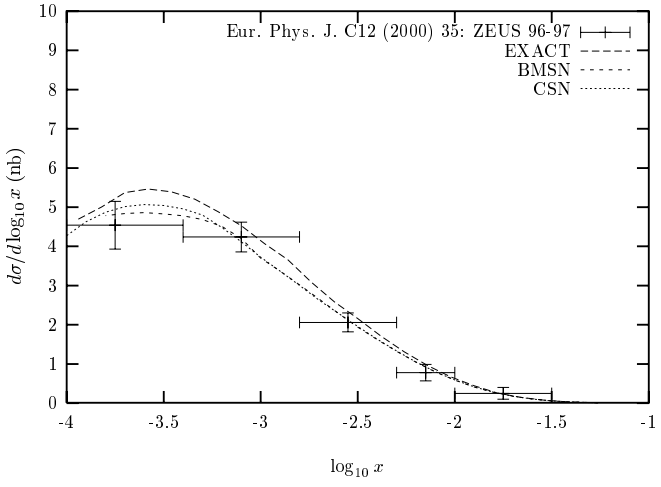

Fig. 9. Same as Fig. 8 displayed on a semi-logarithmic plot

these variables. Contour lines are drawn where this ratio is 1, 1.5, 2, 2.5 and 3. The ratio increases as Q^2 increases for fixed x. Note that no acceptance corrections in p_T or η have been applied to the ratio in this figure. One sees that the region of large Q^2 and large x must be probed to find significant differences between FOPT and the variable flavor number schemes. Roughly speaking one needs $x > 0.2$ and $Q^2 > 100$ GeV^2. In fact Fig. 5 in [32], which only shows the Q^2 dependence of the structure function $F_2^c(x, Q^2, m_c^2)$ at fixed values of x, already illustrates the kind of differences one can expect in this region.

Finally we remark that as far as the FOPT result is concerned the standard version of HVQDIS uses the scale $\mu^2 = Q^2 + 4m_c^2$. This increases the scale in the running coupling. Also it uses the second and third lines of (2.9) with all parton densities set to their three flavor NLO values. These standard settings alter slightly the above acceptance curves. The net effect of both changes is approximately a ten percent reduction of the FOPT results (using GRV98) for the differential distribution in $\log_{10}Q^2$

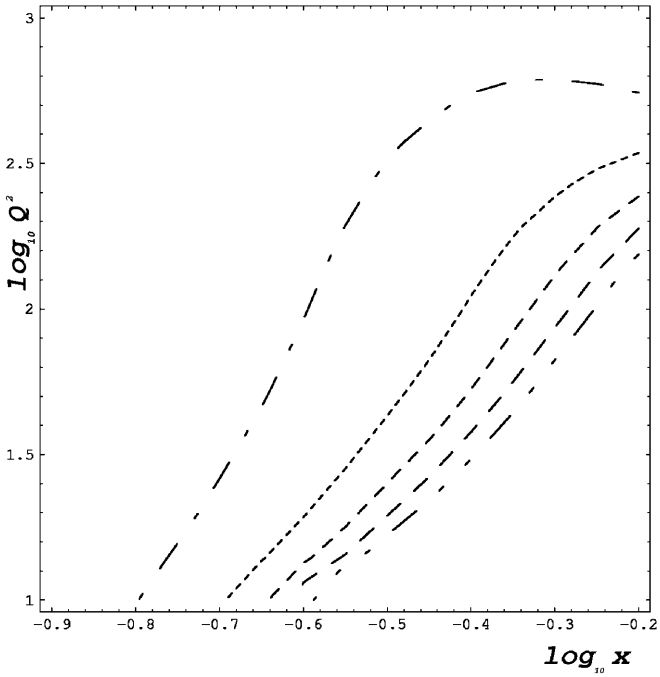

Fig. 10. Ratio of the double differential cross sections in $\log_{10}Q^2$ and $\log_{10}x$ for the BMSN scheme divided by the FOPT result. The contour lines are for the ratio 1, 1.5, 2, 2.5 and 3 in the order of increasing Q^2 for fixed x

at the smallest Q^2, which is within the present experimental errors.

To summarize we have made a first comparison between the FOPT, BMSN and CSN descriptions for $D^{*\pm}$ electroproduction. We have observed that the three schemes give nearly identical predictions up to the highest Q^2 measured. It is therefore difficult to distinguish between the various schemes on the basis of a data comparison. The small scale dependence of the FOPT result indicates that there is no sign that the terms containing powers of $\ln(Q^2/m_c^2)$ destroy the convergence of the QCD perturbation expansion and that one is forced to switch to a variable flavor number scheme like the BMSN or CSN. In fact they all provide a good description of the data for the differential distributions in Q^2 and x. At small Q^2 there is a chance to distinguish between the schemes (say for $2 < Q^2 < 20$ in GeV^2). The comparisons in the case of the x-distributions are not conclusive due to the correlations with the points in small Q^2. It will be interesting to see what happens when more events are collected so that the error bars are reduced.

Acknowledgements. We would like to acknowledge discussions with W. L. van Neerven on the results presented above, and thank José Repond for discussions about the ZEUS data and comments on the text. The work of A. Chuvakin and J. Smith was supported in part by the National Science Foundation Contract PHY-9722101. The work of B. Harris was supported by the U.S. Department of Energy, High Energy Physics Division, under contract W-31-109-Eng-38.

References

1. E. Laenen, S. Riemersma, J. Smith and W. L. van Neerven, Nucl. Phys. **B392**, 162 (1993); ibid. 229 (1993); S. Riemersma, J. Smith and W. L. van Neerven, Phys. Lett. **B347**, 43 (1995)
2. B. W. Harris and J. Smith, Nucl. Phys. **B452**, 109 (1995)
3. B. W. Harris and J. Smith. Phys. Rev. D**57**, 2806 (1998); B. W. Harris, E. Laenen, S. Moch and J. Smith, in Monte Carlo Generators for HERA Physics edited by A. T. Doyle et al., (DESY, Hamburg 1999), p. 464, [hep-ph/9905365]
4. ZEUS Collaboration, J. Breitweg et al., Eur. Phys. J. **C12**, 35 (2000)
5. H1 Collaboration, C. Adloff et al., Nucl. Phys. **B545**, 21 (1999)
6. H1 Collaboration, Abstract 984, Submitted to the XXXth International Conference on High Energy Physics, July 27-August 2, 2000, Osaka, Japan, [http://ichep2000.hep.sci.osaka-u.ac.jp]
7. ZEUS Collaboration, Abstract 855, Submitted to the XXXth International Conference on High Energy Physics, July 27-August 2, 2000, Osaka, Japan, [http://ichep2000.hep.sci.osaka-u.ac.jp]
8. M. Glück, E. Reya and M. Stratmann, Nucl. Phys. **B422**, 37 (1994); A. Vogt in Deep Inelastic Scattering and Related Phenomena, DIS96, edited by G.D. 'Agostini and A. Nigro, (World Scientific 1997), p. 254, [hep-ph/9601352]
9. B. W. Harris in New Trends in HERA Physics 1999 edited by G. Grindhammer et al., (Springer-Verlag, Berlin 2000), p. 290, [hep-ph/9909310]
10. M. Glück, E. Reya and A. Vogt, Eur. Phys. J. **C5**, 461 (1998)
11. M. Buza, Y. Matiounine, J. Smith and W. L. van Neerven, Eur. Phys. J. **C1**, 301 (1998)
12. A. Chuvakin and J. Smith, Phys. Rev. D**61**, 114018 (2000)
13. W. L. van Neerven and E. B. Zijlstra, Phys. Lett. **B272**, 127 (1991); E. B. Zijlstra and W. L. van Neerven, Phys. Lett. **B273**, 476 (1991); Nucl. Phys. **B383**, 525 (1992)
14. M. A. G. Aivazis, J. C. Collins, F. I. Olness and W. -K. Tung, Phys. Rev. D**50**, 3102 (1994); F. I. Olness and S. Riemersma, Phys. Rev. D**51**, 4746 (1995)
15. H. L. Lai, J. Huston, S. Kuhlmann, J. Morfin, F. I. Olness, J. Owens, J. Pumplin and W. -K. Tung, Eur. Phys. J. **C12**, 375 (2000)
16. A. D. Martin, R. G. Roberts, W. J. Stirling and R. Thorne, Eur. Phys. J. **C4**, 463 (1998)
17. M. Krämer, F. I. Olness and D. E. Soper, Phys. Rev. D**62**, 096007 (2000)
18. M. Buza, Y. Matiounine, J. Smith and W. L. van Neerven, Phys. Lett. **B411**, 211 (1997)
19. A. Chuvakin, J. Smith and W. L. van Neerven, Phys. Rev. D**61**, 096004 (2000)
20. W. L. van Neerven, Acta Phys. Polon. **B28**, 2715 (1997); W. L. van Neerven in Proceedings of the 6th International Workshop on Deep Inelastic Scattering and QCD "DIS98" edited by Gh. Coremans and R. Roosen, (World Scientific, 1998), p. 162-166, [hep-ph/9804445]; J. Smith in New Trends in HERA Physics, edited by B. A. Kniehl, G. Kramer and A. Wagner, (World Scientific, 1998), p. 283, [hep-ph/9708212]; J. Smith in the proceedings of the 8th International Workshop on Deep Inelastic Scattering and QCD, (DIS2000), Liverpool, England, 25-30 April 2000, [hep-ph/0005242]

21. R. S. Thorne and R. G. Roberts, Phys. Lett. **B421**, 303 (1998); Phys. Rev. D**57**, 6871 (1998)
22. J. C. Collins, Phys. Rev. D**58**, 0940002 (1998)
23. J. Amundsen, C. Schmidt, W. -K. Tung and X. N. Wang, JHEP 0010, 031 (2000)
24. G. Ingelman, J. Rathsman, and G. A. Schuler, Comput. Phys. Commun. 101, 135 (1997)
25. G. A. Schuler, Nucl. Phys. **B299** 21 (1988)
26. C. Peterson, D. Schlatter, I. Schmidt and P. Zerwas, Phys. Rev. D**27**, 105 (1983)
27. P. Nason and C. Oleari, Nucl. Phys. **B565**, 245 (2000)
28. L. Gladilin, [hep-ex/9912064]
29. E. Norrbin and T. Sjostrand, in Monte Carlo Generators for HERA Physics edited by A. T. Doyle et al., (DESY, Hamburg 1999), p. 506, [hep-ph/9905493]
30. T. Sjostrand, Comput. Phys. Commun. **82**, 74 (1994); H. Jung, Comp. Phys. Commun. **86**, 147 (1995)
31. A. Chuvakin, J. Smith and W. L. van Neerven, Phys. Rev. D**62**, 036004 (2000)
32. J. Smith in New Trends in HERA Physics, edited by B. A. Kniehl, G. Kramer and A. Wagner, (World Scientific, 1998), p. 283, [hep-ph/9708212]